RSC Medicinal Chemistry

ROYAL SOCIETY OF CHEMISTRY

RESEARCH ARTICLE

View Article Online
View Journal | View Issue

Cite this: *RSC Med. Chem.*, 2024, **15**, 1929

Benzenesulfonamide decorated dihydropyrimidin(thi)ones: carbonic anhydrase profiling and antiproliferative activity†

Hakan Aslan, *[ab] Gioele Renzi,[b] Andrea Angeli, [b] Ilaria D'Agostino, *[bc] Roberto Ronca, [d] Maria Luisa Massardi, [d] Camilla Tavani, [d] Simone Carradori, [e] Marta Ferraroni, [f] Paolo Governa, [g] Fabrizio Manetti, [g] Fabrizio Carta *[b] and Claudiu T. Supuran [b]

In the last decades, carbonic anhydrases (CAs) have become the top investigated innovative pharmacological targets and, in particular, isoforms IX and XII have been widely studied due to the evidence of their overexpression in hypoxic tumors. The frantic race to find new anticancer agents places the quick preparation of large libraries of putative bioactive compounds as the basis of a successful drug discovery and development programme. In this context, multi-component and, in general, one-step reactions are becoming very popular and, among them, Biginelli's reaction gave clean and easy-to-isolate products. Thus, we synthesized a series of Biginelli's products (**10–17a–b**) and similar derivatives (**20–21**) bearing the benzenesulfonamide moiety, which is known to inhibit CA enzymes. Through the stopped-flow technique, we were able to assess their ability to inhibit the targeted CAs IX and XII in the nanomolar range with promising selectivity over the physiologically relevant isoforms I and II. Crystallography studies and docking simulations helped us to gain insight into the interaction patterns established in the enzyme–inhibitor complex. From a chemical similarity-based screening of in-house libraries of compounds, a diphenylpyrimidine (**23**) emerged. The surprisingly potent inhibitory activity of **23** for CAs IX and XII along with its strong antiproliferative effect on two (triple-negative breast cancer MDA-MB-231 and glioblastoma U87MG) cell lines laid the foundation for further investigation, again confirming the key role of CAs in cancer.

Received 9th February 2024,
Accepted 24th March 2024

DOI: 10.1039/d4md00101j

rsc.li/medchem

Introduction

Cancer is one of the leading causes of mortality worldwide[1,2] and a disease that mostly impacts negatively on the quality of life of the patients and their families along with the public costs.[3] The entire scientific community, both the pharma industry and academia, is frantically searching for new therapeutical options through the application of recently developed technologies, *e.g.*, CRISPR gene editing,[4,5] robotic surgery,[6] personalized medicine,[7] and the generation of new drugs from chemical, natural, and biotechnological sources.[8] Undoubtedly, the most chosen approach is based on the discovery and validation of new putative pharmacological targets, *e.g.* enzymes, receptors, and microRNAs,[9] through a complex multidisciplinary study, often including artificial intelligence,[10] in order to escape (multi)drug-resistance phenomena and reduce the risk of collateral effects that lower significantly the patient compliance.

In the last decades, some of us shed light on the roles and functions of the superfamily of carbonic anhydrases (CAs, EC 4.2.1.1) in relevant physiological processes in prokaryotes and eukaryotes by means of the reversible hydration of carbon dioxide (CO_2).[11] Eight genetic families (α, β, δ, ε, ζ, η, θ, and ι) have been reported to date, with human (h) genome encoding for 15 isoforms belonging to the α-class.[12] Their druggability has been already proved and several modulators,

[a] *Department of Chemistry, Faculty of Science and Arts, Sinop University, Sinop, Turkey. E-mail: hakaslan@gmail.com*
[b] *NEUROFARBA Department, Sezione di Scienze Farmaceutiche, University of Florence, Sesto Fiorentino, Florence, 50019, Italy. E-mail: fabrizio.carta@unifi.it*
[c] *Department of Pharmacy, University of Pisa, 56126, Pisa, Italy. E-mail: ilaria.dagostino@unipi.it*
[d] *Department of Molecular and Translational Medicine, University of Brescia, 25123 Brescia, Italy*
[e] *Department of Pharmacy, "G. d'Annunzio" University of Chieti-Pescara, 66100 Chieti, Italy*
[f] *Department of Chemistry "Ugo Schiff", University of Florence, Sesto Fiorentino, Florence, 50019, Italy*
[g] *Department of Biotechnology, Chemistry and Pharmacy, University of Siena, 53100, Siena, Italy*

† Electronic supplementary information (ESI) available: Chemistry, heat map for selectivity indexes, electron density maps of inhibitor **12a**, chemistry – experimental, NMR spectra of final compounds. See DOI: https://doi.org/10.1039/d4md00101j

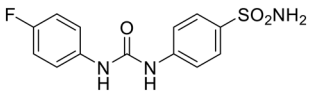

SLC-0111

Fig. 1 Structure of licensed **SLC-0111**.

both inhibitors and activators,[11] have been developed, with some compounds reaching (pre)clinical use, such as diuretics, anti-glaucoma, anti-obesity, and anti-epileptic agents,[13] owing to the smart tail approach.[14,15] In this context, the transmembrane hCAs IX and XII could be listed as the most promising anticancer targets.[16–21] These isoforms are overexpressed in several solid tumors, *e.g.*, breast, lung, and colorectal, by the hypoxia-inducible factors (HIF-1α and -2α), allowing the maintenance of the optimal pH for cell survival in hypoxic conditions and also contributing to cancer cell migration, invasion, and stemness.[16] Selective inhibition of the two isoenzymes was reported to impair their functionality, causing the cancer cell to undergo apoptosis *in vitro* on a large panel of cancer cell lines[22–24] and *in vivo* in xenograft tumor models.[25,26] For instance, a small molecule containing the prototypic benzenesulfonamide CA inhibitor **SLC-0111** (Fig. 1) was developed and is currently under clinical trial in combination with gemcitabine for metastatic pancreatic ductal adenocarcinoma.[27,28]

Moreover, the continuous race to quickly find new active molecules with chemical diversity leads researchers to generate large libraries through easy synthetic schemes, often by just one-step procedures. In particular, multi-component reactions, such as Biginelli,[29] could represent a good strategy that allows practically performing small chemical changes, employing just one different chemical per time, and, thereby, conducting easily but robust structure–activity relationships (SARs).[30–34] Indeed, Biginelli's reaction permits the high-yielding obtainment of 3,4-dihydropyrimidin-2-(1*H*)-ones and -thiones (DHPMs)[35] by reacting the suitable urea or thiourea with an aromatic aldehyde and a β-ketocarboxyl derivative.

Results

Chemistry

DHPMs **10–17a–b** were synthesized through Biginelli's three-component reaction, as depicted in Scheme 1, by using 4-formyl benzenesulfonamide **1** (previously prepared as reported in Scheme S1 in ESI†),[36,37] the suitable active methylene-containing derivatives **2–9**, and urea or thiourea in the presence of sodium hydrogen sulfate ($NaHSO_4$).[38]

Compounds **2–6** were commercially available, while **7–9** were prepared by us, as reported in ESI† (Schemes S2 and S3).[39,40] Instead, pyrimidintriones **20–21** were obtained *via* condensation (Scheme 1), by reacting aldehyde derivative **1** with compounds **18** and **19**.

Compound **23** was obtained in a straightforward synthetic pathway by first reacting intermediate **1** with acetophenone to afford chalcone **22**, which in turn was cyclized with

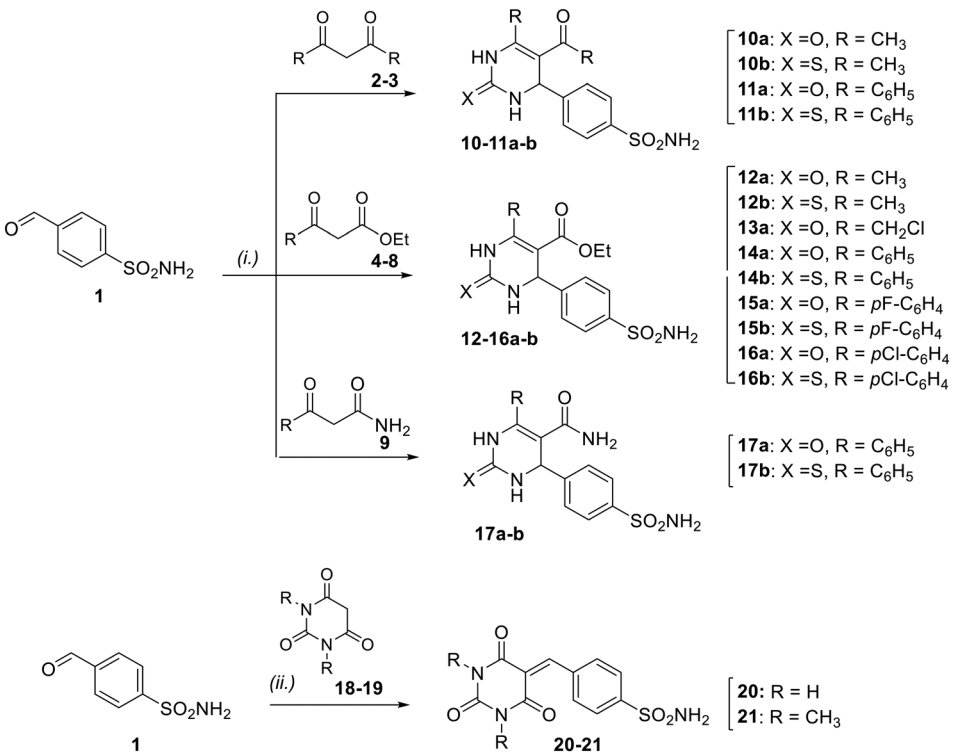

Scheme 1 Synthetic pathway for the target compounds **10–17a–b**, **20** and **21**. Reagents and conditions: i) urea (for compounds **10–17a**) or thiourea (for compounds **10–12b** and **14–17b**), $NaHSO_4$, hexane/ACN, reflux, 6–24 h; ii) NaOH aq., EtOH, 0 °C–r.t., 16 h.

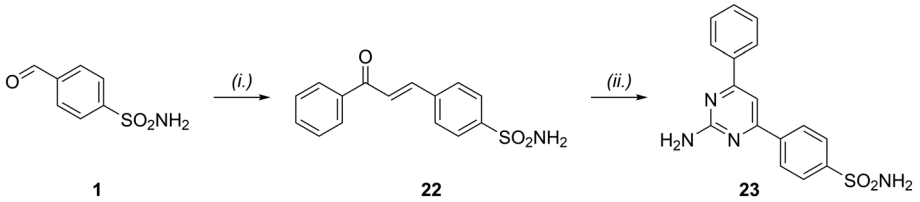

Scheme 2 Synthesis of 2-aminopyrimidine **23**. Reagents and conditions: i) acetophenone, NaOH aq., EtOH, 0 °C–r.t., 16 h; ii) guanidine hydrochloride, EtOH, KOH aq.; then, 30% H_2O_2 aq., refl., 16 h.

guanidine and oxidated by 30% H_2O_2 aq. through a two-step-one-pot reaction (5) (Scheme 2).

Enzymatic evaluation on human carbonic anhydrases

The inhibition profiles of **10–12a–b**, **13a**, **14–17a–b**, **20**, **21**, and **23** on the abundantly expressed hCAs I and II, the central nervous system (CNS)-associated hCA VII, and the hypoxic-tumor-associated hCAs IX and XII were determined through the stopped-flow CO_2 hydrase assay.[41] Inhibition constants (K_I) are reported in Table 1 with the reference compound acetazolamide (**AAZ**).

Overall, inhibition data in Table 1 showed that most of the obtained derivatives were remarkably selective for hCAs IX and XII, resulting in nanomolar inhibitors. In some cases, subnanomolar K_I values were found for hCA II (*i.e.*, **11b** and **12b**). The following SARs are reported for hCAs I and II and tumoral isoforms IX and XII, while a separate section is dedicated to data on the VII isoenzymes.

The introduction of the isosteric sulfur atom within the 5-acetyl-6-methyl-2-oxo-1,2,3,4-tetrahydropyrimidin-4-yl moiety in **10a** to afford **10b** improved the inhibitory activity towards the isoforms I, II and IX by 4.0-, 1.5- and 4.8-fold, respectively, while a slight (1.3-fold) K_I value increase was noticed for the other tumor-associated isoform.

A different kinetic pattern was observed when the same substitution was performed on the 5-acetyl-6-phenyl-2-oxo-1,2,3,4-tetrahydropyrimidin-4-yl moiety in **11a**. In this case, the thiooxo derivative **11b** was a more potent inhibitor than its parent compound only against hCAs I and II (by 2.3- and 19.3-fold, respectively), whereas very slight K_I variations were registered against the other isoforms.

As for the ethyl ester **12a**, a consistent increase of the inhibitory potency was observed only for hCAs II and XII by 76- and 1.8-fold, respectively, while the K_I value for hCA I was enhanced by 4.2-fold. Quite interestingly, hCA IX was not affected by the O-S substitution (K_Is of 8.9 and 8.1 for **12a** and **12b**, respectively). The same isosteric substitution was explored for **14–17a–b** and different SAR considerations could be generated.

For instance, the replacement of the methyl group at position 6 in the tetrahydropyrimidine ring in **12a** with a phenyl group (**14a**) induced a relevant increase in the inhibitory potency for hCAs I and II by 4.2- and 31.1-fold, respectively (K_Is = 16.1 and 2.1 nM). Conversely, the tumor-associated IX and XII isoforms resulted in a far weak inhibition by 4.0- and 9.6-fold, respectively (K_Is of 36.0 and 594 nM). Interestingly, the thiooxo derivative of **14a**, namely **14b**, induced an opposite kinetic pattern with the K_I values for hCAs I and II of 643 and 91.0 nM, respectively, thus with a 39.9- and 43.3-fold increase. On the other hand, hCAs IX and XII resulted to be 7.5- and 6.6-fold more potently inhibited (K_Is of 4.8 and 89.7 nM), respectively.

The introduction of the fluorine and chlorine atoms in **14a** to afford **15a** and **16a**, respectively, clearly induced substantial changes in the *in vitro* kinetics. Data in Table 1 showed that the fluoro raised the K_I values for hCAs I and II by 16.9- and 7.9-fold, respectively, and, conversely, the affinity for the tumor-associated isoforms by 1.2- and 2.0-fold. A similar kinetic trend was reported when the choro atom in **15a** was placed instead (**16a**). Noteworthily, such a halogen showed a less significant reduction of the ligand affinity for hCAs I and II when compared to that of **15a** with respect to the unsubstituted progenitor **14a**. On the other hand, the inhibitory potency of the chloro-containing **16a** on the tumor-associated hCAs was highly enhanced up to low nanomolar values (7.3 and 9.7 nM, respectively). It is of interest that the manipulation of our derivatives with halogens, although at a very simple level, had a great impact on the potency and selectivity of the ligands against the various isozymes considered. Again, the isosteric substitution of the oxygen in **15a** and **16a** with sulfur instead, as in **15b** and **16b**, showed significant K_I variations. As reported in Table 1, the inhibitory potency of **15b** against hCAs I and XII was enhanced by 2.9- and 4.0-fold, respectively, when compared to its oxo progenitor **15a** (K_Is for **15a** = 272 and 289 nM for hCAs I and XII, respectively; K_Is for **15b** = 95 and 72 nM for hCAs I and XII, respectively). On the contrary, the inhibitory potency of **15b** against the remaining isoforms II and IX decreased by 3.5- and 1.7-fold, respectively. As regards **16b**, a specific kinetic trend was reported for all the investigated hCAs, with all K_I values enhanced when compared to the progenitor **16a**.

The introduction of the carboxamide at position 5 of the 6-phenyl-tetrahydropyrimidine ring as in **17a** induced a significative and selective inhibition of the tumor-associated isoforms IX and XII (K_Is of 6.6 and 8.9 nM, respectively) over the ubiquitous hCAs I and II (K_Is of 217 and 70.5 nM, respectively). The isosteric manipulation performed on **17a** to afford **17b** maintained the kinetic trend and, specifically, spoiled the K_I values for hCAs I, II, and IX but resulted in being ineffective for the isoform XII.

Table 1 Inhibition data of sulfonamides **10–12a**, **12b**, **13a**, **14–17a–b**, **20**, **21**, **23** and reference compound **AAZ** on hCAs I, II, VII, IX, and XII through the stopped-flow CO_2 hydrase assay[41]

Compounds	K_I (nM)[a]				
	hCA I	hCA II	hCA VII	hCA IX	hCA XII
10a	362	45.9	19.7	39.0	7.7
10b	91.4	31.4	63.8	8.1	9.8
11a	265	5.6	12.3	7.9	10.6
11b	116	0.29	14.5	9.9	9.2
12a	68.0	65.3	25.7	8.9	61.7
12b	286	0.86	15.5	8.1	33.6
13a	630	43.8	18.5	3.5	8.5
14a	16.1	2.1	10.1	36.0	594
14b	643	91.0	191	4.8	89.7
15a	272	16.6	102	30.5	289
15b	95.0	58.2	168	52.2	72.0
16a	22.8	8.4	25.0	7.3	9.7
16b	760	25.2	17.8	56.5	34.1
17a	217	70.5	88.0	6.6	8.9
17b	491	200	18.1	41.3	8.7
20	957	29.1	202	7.1	57.8
21	97.0	17.3	9.1	8.2	100
23	621	377	433	8.9	5.3
AAZ	250	12.1	2.5	25.8	5.7

[a] Mean from 3 different assays by a stopped-flow technique (errors were in the range of ±5–10% of the reported values).

Similar SARs were obtained for pyrimidintrione derivatives **20** and **21** and a preferential inhibition of hCAs II and IX was clearly observed in both cases. Methyl substitutions on the pyrimidine moiety in **20** greatly enhanced the binding affinity for hCA I (K_Is = 957 and 97 nM for **20** and **21**, respectively), and slightly affected that for hCA II (K_Is = 29.1 and 17.3 nM for **20** and **21**, respectively). Conversely, such a structural modification reduced the inhibitory potency for the tumor-associated IX and XII isoforms, with the latter being particularly affected (by 1.7-fold).

Among the series, 6-(chloromethyl)-tetrahydropyrimidine **13a** and 2-aminopyrimidine **23** have structural peculiarities that set them apart. Besides such differences, both **13a** and **23** shared similar kinetic preferentiality for hCAs IX and XII over the I and II isoforms. Among them, a slight selectivity was reported, with **13a** being 2.4-fold more potent against hCA IX than against the isoform XII (K_Is = 3.5 and 8.5 nM, respectively), whereas **23** was 1.7-fold more potent against hCA XII than against the isoform IX (K_Is of 8.9 and 5.3 nM, respectively).

As for the CNS-associated hCA VII, isosteric substitution on **10a** by the introduction of the sulfur atom was proved to be detrimental to the inhibitory potency (K_Is = 19.7 and 63.8 nM for **10a** and **10b**, respectively). The same *in vitro* kinetic trend was reported for **11a** and **11b**, although with moderate intensity (K_Is = 12.3 and 14.5 nM, respectively). Among the 5-ethyl ester-tetrahydropyrimidin-4-yl containing moiety series, the thiooxo derivative **12b** was 1.7-fold more potent than its precursor **12a** (K_Is = 15.5 and 25.7 nM for **12b** and **12a**, respectively). On the other hand, 6-phenyl derivative **14b** was a 18.9-fold weaker inhibitor of hCA VII when compared to **14a**, with K_Is equal to 191 and 10.1 nM, respectively. The halogen effect was clearly shown also for the hCA VII *in vitro* kinetics. For instance, the introduction of the fluorine and chlorine atoms in **14a** to afford **15a** and **16a**, respectively, spoiled the inhibitory potency by 10.0- and 2.5-fold (K_Is = 102 and 25.0 nM for **15a** and **16a**), respectively. Quite interestingly, the sulfur isosteric manipulation on **14a** and **15a** heavily affected their K_I values, which were raised by 18.9- and 1.6-fold for **14b** and **15b**, respectively. A slight improvement (by 1.4-fold) of the binding affinity was observed for **16b** compared to its precursor **16a** (K_Is = 25.0 and 17.8 nM for **16a** and **16b**, respectively). Also, a notable increase in inhibitory potency on hCA VII was observed for thiooxo **17b** when compared to its oxo progenitor (K_Is = 88.0 and 18.1 nM for **17a** and **17b**, respectively).

Among the pyrimidintriones **20** and **21**, the methyl substitution produced a remarkable enhancement of the inhibitory potency up to 22.2-fold. Finally, **13a** and **23** showed K_I values equal to 18.5 and 433 nM, respectively.

The selectivity index (SI) for each compound was calculated and a heat map is reported in ESI† (Fig. S1). In general, a good SI can be observed for the whole library of compounds over hCA I and hCA VII, while they were potent also against hCA II, apart from compound **14a**, which preferentially inhibits the physiologically relevant isoforms I and II. Notably, compounds **10b** and **17a** were found to be the most selective in the series, with the latter showing a high selectivity for hCA IX (SI in the range of 10–100). Finally, compound **23** emerged as a selective inhibitor of tumor-associated isoforms, with a SI value >10.

Crystallographic data

We conducted an X-ray crystallographic investigation to decipher the binding mode of representative compounds of the series within the active site of hCAs considered in this study. Tetrahydropyrimidine **12a** was the only one that afforded an adduct with the isoform I stable enough to be considered for our purposes.[42] In addition, such an isoform is highly prevalent in red blood cells at a relevant concentration (*i.e.*, up to 1 μM) and, thus, retains high value in pharmacokinetics. The electron density map revealed the presence of the inhibitor within the hCA I active site, clearly attributable to compound **12a** (Fig. S2 in ESI†). This binding mode is facilitated by the interaction between the primary sulfonamide group in its anionic form and the protein Zn^{2+} ion (Fig. 2).

The inhibitor also forms a robust hydrogen bond between one oxygen atom of the sulfonamide group and the amide nitrogen of Thr199. This coordination pattern is consistent with the typically reported primary sulfonamides.[42] Furthermore, the inhibitor is firmly stabilized within the active site through several interactions. There is a T-shaped π-stacking interaction between the phenyl ring and His94 at the base of the cavity. Additionally, a hydrophobic interaction occurs with the side chain of Leu198 (Fig. 2). The inhibitor

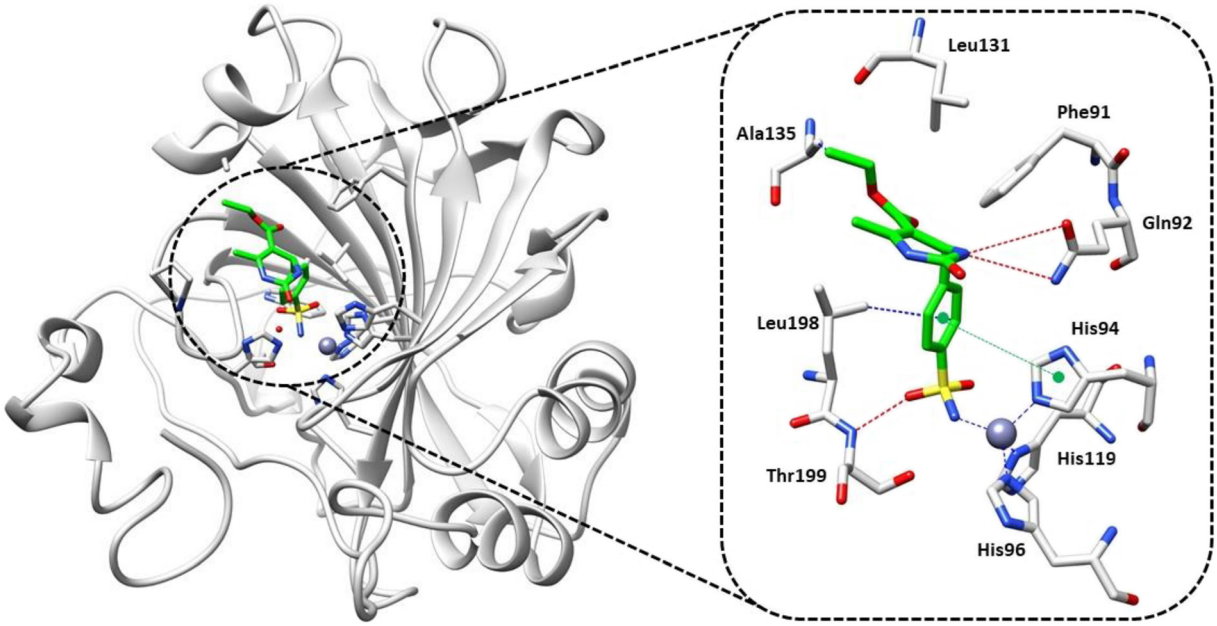

Fig. 2 hCA I in complex with **12a**. residues involved in the binding of inhibitors are also shown; the grey sphere represents the zinc ion within the enzyme active site. Interactions between the inhibitor and enzyme residues are also shown: blue hydrophobic interactions; red hydrogen bonds; and green π–π stacking interactions.

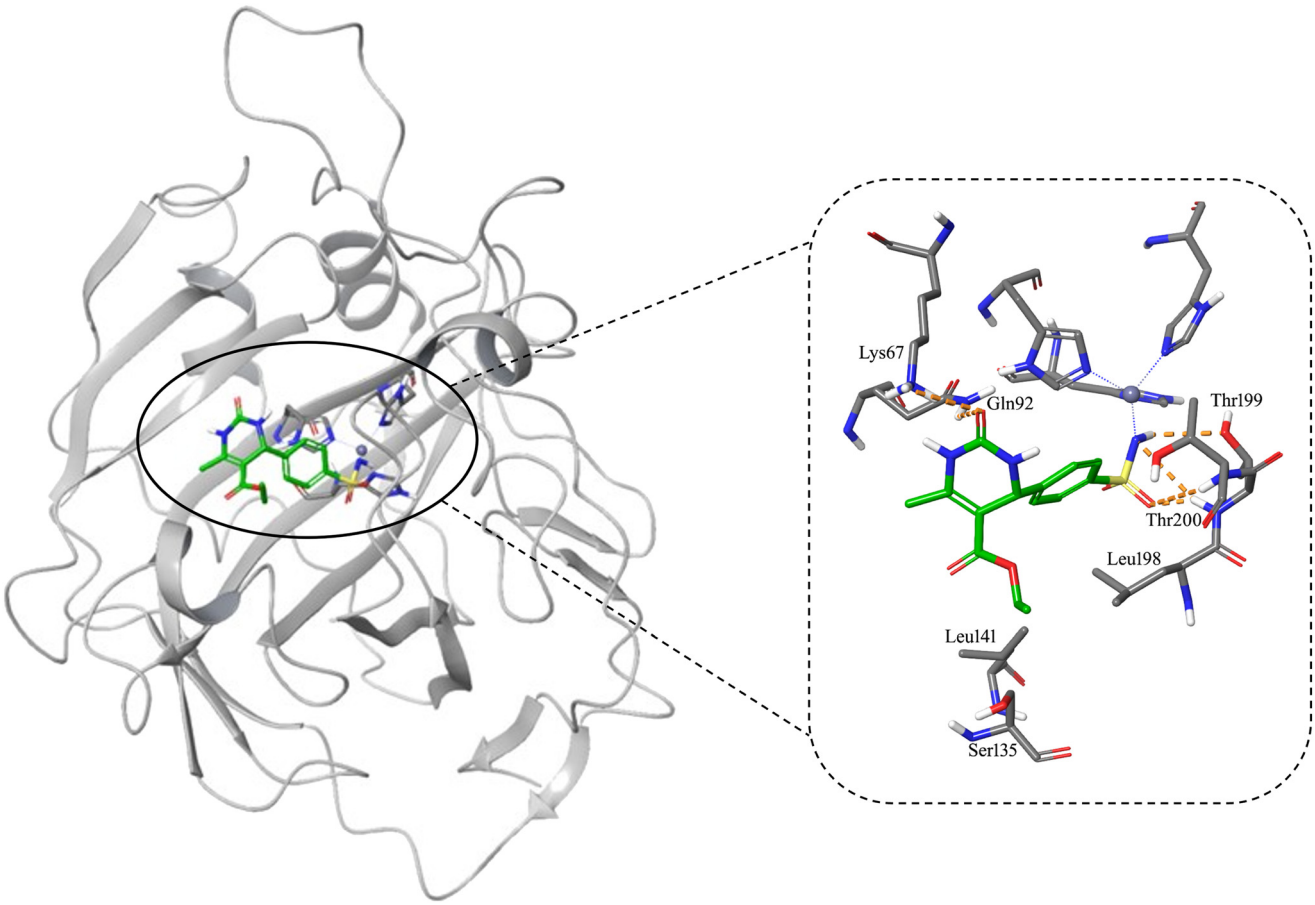

Fig. 3 Graphical representation of the best-scored pose of **12a** (green carbon atoms and atom type notation) within the binding site of hCA XII (PDB ID: 6YH9). For the sake of clarity, only amino acids important for binding interactions are shown, in addition to his residues and zinc ion (blue sphere) of the catalytic machinery. Hydrogen bonds are represented by orange dotted lines.

tail in **12a** is engaged in hydrophobic interactions with Ala135 and forms two hydrogen bonds with the side chain of Gln92. Such a dual interaction with Gln92 is probably due to the presence of a keto-enolic equilibrium not clearly observable within the conducted experiments. In Table S1,† a summary of the data collected for cocrystal hCA I and compound **12a** is reported.

Molecular docking simulations on the hCA XII isoform

The three-dimensional structure of hCA XII in complex with a benzenesulfonamide has been used to predict the putative binding mode of **12a** by using Glide software (Maestro suite, Schrodinger). As a result, the best-scored binding pose of **12a** and the co-crystallized ligand showed a similar location and orientation of their common benzenesulfonamide portion, which was predicted in the deprotonated form as the preferred tautomer. In addition to serving as a chelating group for the zinc ion, the sulfonamide group was involved in a network of hydrogen bonds (Fig. 3).

In particular, the NH system is a hydrogen bond donor for the hydroxyl group of the Thr199 side chain, while the amide nitrogen atom served as an acceptor for the backbone NH group of Thr199, which in turn also interacted with one of the sulfone oxygen atoms. An additional hydrogen bond was found between sulfone oxygen and the backbone NH of Thr200. Moreover, the complex was further stabilized by a bifurcated hydrogen bond between the pyrimidone oxygen and the terminal ammonium group of Lys67 and with the NH_2 group of Gln92. Finally, the ethyl group of the ester side chain was accommodated within a hydrophobic cage delimited by the alkyl portions of Leu141, Leu198, and Ser135.

In vitro anti-proliferative activity

Representative compounds **13a**, **17a–b**, and **23** were selected for their potent inhibitory profile on cancer-associated isoforms hCAs IX and XII and their selectivity over the physiologically relevant I and II isoforms. Along with **SLC-0111** (Fig. 1), the antiproliferative effect of the compounds was evaluated on a human triple-negative breast cancer cell line (MDA-MB-231, Fig. 4) and a human glioblastoma cell line (U87MG, Fig. 5) with a high basal expression of hCA IX.[22,43] Thus, the cells were treated with the compounds at different concentrations and their efficacy to inhibit the proliferation was assessed after 72 h of treatment in hypoxic conditions by cytofluorimetric cell count (Fig. 4 and 5). As already reported,[22,43] the reference compound **SLC-0111** was effective in reducing the proliferation of MDA-MB-231 (IC_{50} = 138 μM). Interestingly, **13a** and **23** showed an enhanced antiproliferative effect, with IC_{50} values of 44.4 and 38.8 μM, respectively. Otherwise, a lack of activity was observed for compounds **17a–b** at 300 μM (Fig. 4).

Moreover, as shown in Fig. 5, **SLC-0111** showed an IC_{50} of 58 μM on U87MG cells, while **23** was the most effective (IC_{50} = 34 μM) and an IC_{50} equal to 100 μM was reported for **13a**.

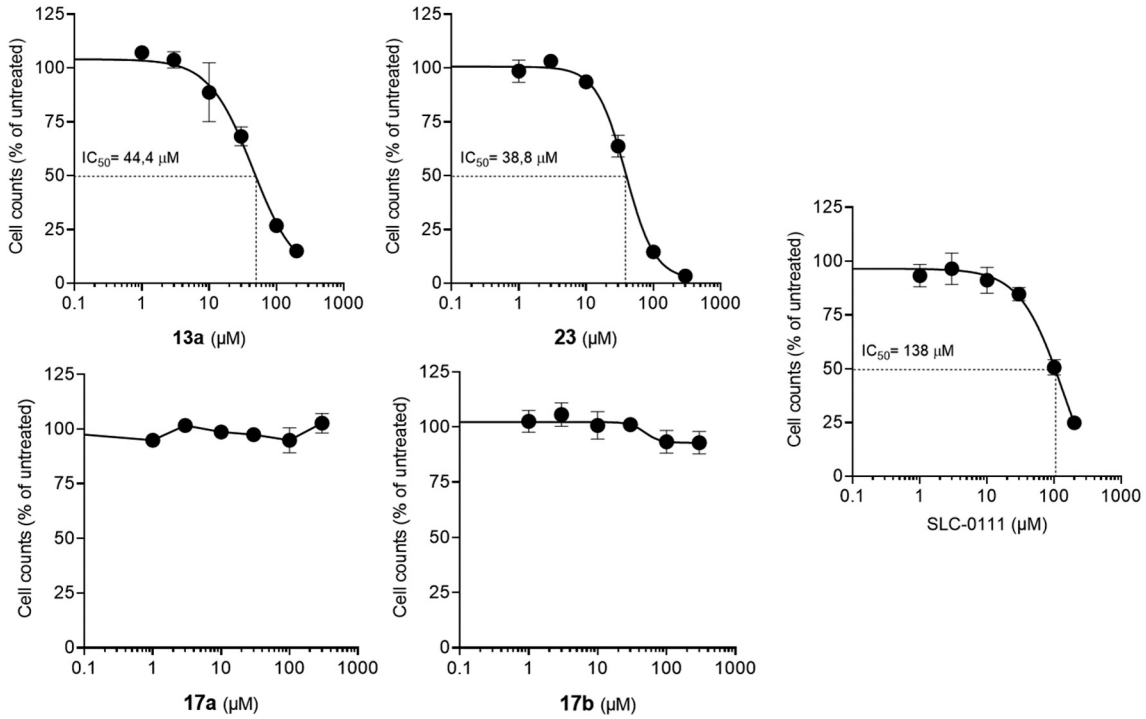

Fig. 4 Cell proliferation of triple-negative breast cancer MDA-MB-231 cells treated for 72 h with **13a**, **17a**, **b**, **23**, or **SLC-0111**. Cell count is referred to the untreated/control considered as 100%.

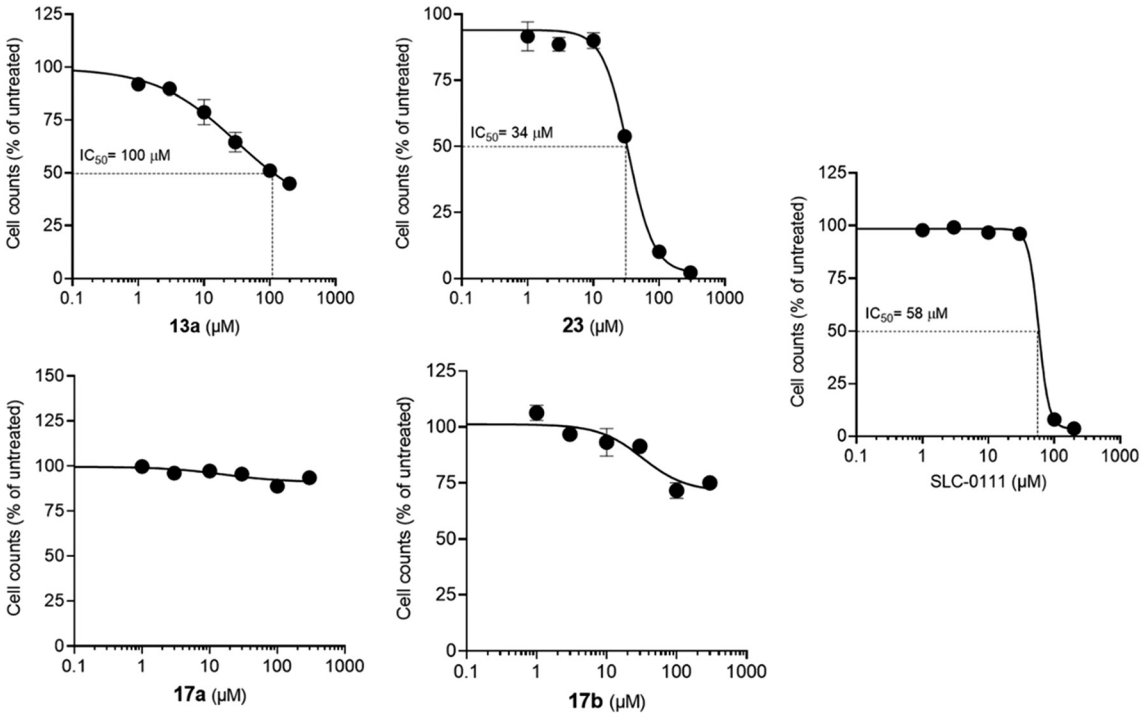

Fig. 5 Cell proliferation of U87MG glioblastoma cells treated for 72 h with **13a**, **17a**, **b**, **23**, or **SLC-0111**. Cell count is referred to the untreated/control considered as 100%. Cell count is referred to the untreated/control considered as 100%.

Once again, **17a–b** showed no relevant antiproliferative activity on the cell line (Fig. 5).

Experimental

Synthesis of the compounds

General chemistry. Anhydrous solvents and all reagents were purchased from Merck, VWR, and TCI. All reactions involving air- or moisture-sensitive compounds were performed under a nitrogen atmosphere. Nuclear magnetic resonance (^{1}H and ^{13}C NMR) spectra were recorded using a Bruker Advance III 400 MHz spectrometer in DMSO-d_6. Chemical shifts are reported in parts per million (ppm) and the coupling constants (J) are expressed in hertz (Hz). Splitting patterns are designated as follows: s, singlet; d, doublet; t, triplet; m, multiplet; brs, broad singlet. The assignment of exchangeable protons (NH) was confirmed by the addition of D_2O. Analytical thin-layer chromatography (TLC) was carried out on Merck silica gel F-254 plates. Flash chromatography purifications were performed on Merck silica gel 60 (230–400 mesh ASTM) as the stationary phase, and EtOAc and hexane were used as eluents. The solvents used in MS measurements were acetone, ACN (Chromasolv grade), purchased from Merck (Milan, Italy), and mQ water 18 MΩ, obtained from Millipore's Simplicity system (Milan, Italy). The mass spectra were obtained using a Varian 1200L triple quadrupole system (Palo Alto, CA, USA) equipped with an electrospray source (ESI) operating in both positive and negative ions. Stock solutions of analytes were prepared in acetone at 1.0 mg mL^{-1} and stored at 4 °C. Working solutions of each analyte were freshly prepared by diluting stock solutions in a mixture of mQ H_2O/ACN 1/1 (v/v) up to a concentration of 1.0 μg mL^{-1}. The mass spectra of each analyte were acquired by introducing, *via* a syringe pump at 10 L min^{-1}, the working solution. Raw data were collected and processed using Varian Workstation version 6.8 software.

Synthetic procedures

*General procedure for the synthesis of DHPM-benzenesulfonamide **10–17a–b**.* A mixture of 4-formyl benzenesulfonamide (0.5 mmol), suitable β-dicarbonyl compounds (0.5 mmol), urea or thiourea (0.6 mmol), and $NaHSO_4$ (1.5 mmol) in hexane/ACN (2.5 : 0.5 mL) was refluxed for 6–24 h. The progress of the reaction was monitored by TLC. After completion, the reaction mixture was cooled to r. t., and H_2O (5 mL) was added. The obtained precipitate was filtered and washed with cold water and Et_2O. The crude product was purified by column flash chromatography on silica gel using hexane/EtOAc 1 : 1 as the eluent.[38]

*4-(5-Acetyl-6-methyl-2-oxo-1,2,3,4-tetrahydropyrimidin-4-yl) benzenesulfonamide (**10a**).* Yield 46%; yellow solid; mp: 237–238 °C; ^{1}H NMR (400 MHz, DMSO-d_6) δ: 2.19 (3H, s, –CH_3), 2.34 (3H, s, –CH_3), 5.36 (1H, d, J = 2.8 Hz, H–C_4), 7.35 (2H, s, –NH_2), 7.44 (2H, d, J = 8.4 Hz), 7.80 (2H, d, J = 8.4 Hz), 7.95 (1H, s, –NH), 9.31 (1H, s, –NH) ppm; ^{13}C NMR (100 MHz, DMSO-d_6) δ: 20.1(CH_3), 31.6 (CH_3), 54.4 (CH), 110.6 (C), 127.1 (CH ×2), 128.0 (CH ×2), 144.1 (C), 149.1 (C), 149.8 (C), 153.1 (C═O), 195.1 (C═O) ppm; LC-MS (ESI) (m/z) 310.2 [M + H]$^+$.

*4-(5-Acetyl-6-methyl-2-thioxo-1,2,3,4-tetrahydropyrimidin-4-yl) benzenesulfonamide (**10b**).* Yield 32%; orange solid; mp: 218–219 °C; ^{1}H NMR (400 MHz, DMSO-d_6) δ: 2.24 (3H, s, –CH_3),

2.39 (3H, s, $-CH_3$), 5.39 (1H, d, J = 3.6 Hz, H–C4), 7.37 (2H, s, $-NH_2$), 7.43 (2H, d, J = 8.4 Hz), 7. 83 (2H, d, J = 8.4 Hz), 9.87 (1H, s, –NH), 10.42 (1H, s, –NH) ppm; ^{13}C NMR (100 MHz, DMSO-d_6) δ: 19.4 (CH_3), 31.7 (CH_3), 54.4 (CH), 111.4 (C), 127.2 (CH ×2), 128.1 (CH ×2), 144.4 (C), 146.2 (C), 147.6 (C), 175.4 (C═S), 195.7 (C═O) ppm; LC-MS (ESI) (m/z): 326.2 $[M + H]^+$.

*4-(5-Benzoyl-2-oxo-6-phenyl-1,2,3,4-tetrahydropyrimidin-4-yl) benzenesulfonamide (**11a**).* Yield 33%; off-white solid; mp: 267 °C (dec.); ^{1}H NMR (400 MHz, DMSO-d_6) δ: 5.43 (1H, d, J = 3.2 Hz, H–C4), 7.04 (2H, t, J = 7.6 Hz), 7.10 (2H, t, J = 7.6 Hz), 7.15–7.19 (2H, m), 7.24 (2H, d, J = 7.2 Hz), 7.29 (2H, d, J = 7.2 Hz), 7.36 (2H, s, $-NH_2$), 7.66 (2H, d, J = 8.0 Hz), 7.86 (2H, d, J = 8.0 Hz), 8.12 (1H, d, J = 3.2 Hz, –NH), 9.56 (1H, bs, –NH) ppm; ^{13}C NMR (100 MHz, DMSO-d_6) δ: 56.2 (CH), 109.7 (C), 127.0 (CH ×2), 128.2 (CH ×2), 128.5 (CH ×2), 128.8 (CH ×2), 129.6 (CH ×2), 130.8 (CH ×2), 130.9 (CH), 131.7 (CH), 134.3 (C), 140.5 (C), 144.1 (C), 148.9 (C), 150.2 (C), 153.5 (C═O), 195.7 (C═O) ppm; LC-MS (ESI) (m/z): 434.2 $[M + H]^+$.

*4-(5-Benzoyl-6-phenyl-2-thioxo-1,2,3,4-tetrahydropyrimidin-4-yl)benzenesulfonamide (**11b**).* Yield 75%; yellow solid; mp: 165–166 °C; ^{1}H NMR (400 MHz, DMSO-d_6) δ: 5.43 (1H, d, J = 2.8 Hz, H–C4), 7.05–7.21 (6H, m), 7.25 (2H, d, J = 7.2 Hz), 7.32 (2H, d, J = 7.6 Hz), 7.38 (2H, s, $-NH_2$), 7.65 (2H, d, J = 8.0 Hz), 7.89 (2H, d, J = 8.4 Hz), 10.01 (1H, s, –NH), 10.74 (1H, bs, –NH) ppm; ^{13}C NMR (100 MHz, DMSO-d_6) δ: 56.0 (CH), 110.3 (C), 127.2 (CH ×2), 128.2 (CH ×2), 128.6 (CH ×2), 128.8 (CH ×2), 129.6 (CH ×2), 131.1 (CH ×2), 131.7 (C), 132.1 (CH), 133.3 (CH), 139.9 (C), 144.4 (C), 146.9 (C), 147.5 (C), 176.2 (C═S), 195.7 (C═O) ppm; LC-MS (ESI) (m/z): 450.2 $[M + H]^+$.

*Ethyl 6-methyl-2-oxo-4-(4-sulfamoylphenyl)-1,2,3,4-tetrahydropyrimidine-5-carboxylate (**12a**).* Yield 65%; pale yellow solid; mp: 258–259 °C; ^{1}H NMR (400 MHz, DMSO-d_6) δ: 1.14 (3H, t, J = 6.8 Hz, CH_2–$\underline{CH_3}$), 2.30 (3H, s, $-CH_3$), 4.02 (2H, q, J = 6.8 Hz, $-CH_2$), 5.24 (1H, s, H–C4), 7.36 (2H, s, $-NH_2$), 7.44 (2H, d, J = 7.2 Hz), 7.81 (2H, d, J = 7.2 Hz), 7.87 (1H, s, –NH), 9.34 (1H, s, –NH) ppm; ^{13}C NMR (100 MHz, DMSO-d_6) δ: 15.1 (CH_3), 18.9 (CH_3), 54.8 (CH), 60.4 (CH_2), 99.6 (C), 127.0 (CH ×2), 127.9 (CH ×2), 144.1 (C), 149.5 (C), 150.0 (C), 153.00 (C═O), 166.2 (C═O) ppm; LC-MS (ESI) (m/z): 340.1 $[M + H]^+$.

*Ethyl 6-methyl-4-(4-sulfamoylphenyl)-2-thioxo-1,2,3,4-tetrahydropyrimidine-5-carboxylate (**12b**).* Yield 69%; white solid; mp: 224–225 °C; ^{1}H NMR (400 MHz, DMSO-d_6) δ: 1.12 (3H, t, J = 7.2 Hz, CH_2–$\underline{CH_3}$), 2.32 (3H, s, CH_3), 4.03 (2H, q, J = 7.2 Hz), 5.25 (1H, s, H–C4), 7.34 (2H, s, $-NH_2$), 7.41 (2H, d, J = 8.4 Hz), 7.82 (2H, d, J = 8.4 Hz), 9.72 (1H, s, –NH), 10.43 (1H, s, –NH) ppm; ^{13}C NMR (100 MHz, DMSO-d_6) δ: 15.1 (CH_3), 18.3 (CH_3), 54.8 (CH), 60.8 (CH_2), 101.1 (C), 127.2 (CH ×2), 128.1 (CH ×2), 144.4 (C), 146.7 (C), 148.0 (C), 166.0 (C═O), 175.4 (C═S) ppm; LC-MS (ESI) (m/z): 356.2 $[M + H]^+$.

*Ethyl 6-(chloromethyl)-2-oxo-4-(4-sulfamoylphenyl)-1,2,3,4-tetrahydropyrimidine-5-carboxylate (**13a**).* Yield 72%; white solid; mp: 204–205 °C; ^{1}H NMR (400 MHz, DMSO-d_6) δ: 1.17 (3H, t, J = 7.2 Hz, $-CH_3$), 4.09 (2H, q, J = 7.2 Hz, $-\underline{CH_2}CH_3$), 4.60 (1H, d, J = 10.8 Hz, $-C\underline{H_a}H_bCl$), 4.83 (1H, d, J = 11.2 Hz, $-CH_a\underline{H_b}Cl$), 5.30 (1H, d, J = 2.8 Hz, H–C4), 7.37 (2H, s, $-NH_2$), 7.46 (2H, d, J = 8.4 Hz), 7.83 (2H, d, J = 8.4 Hz), 7.98 (1H, bs, –NH), 9.63 (1H, s, –NH) ppm; ^{13}C NMR (100 MHz, DMSO-d_6) δ: 15.0 (CH_3), 40.3 (CH_2), 54.7 (CH), 61.2 (CH_2), 102.1 (C), 127.1 (CH ×2), 127.9 (CH ×2), 144.4 (C), 147.7 (C), 148.6 (C), 152.9 (C═O), 165.1 (C═O) ppm; LC-MS (ESI) (m/z): 374.1 $[M + H]^+$.

*Ethyl 2-oxo-6-phenyl-4-(4-sulfamoylphenyl)-1,2,3,4-tetrahydropyrimidine-5-carboxylate (**14a**).* Yield 34%; yellow solid; mp: 236–237 °C; ^{1}H NMR (400 MHz, DMSO-d_6) δ: 0.75 (3H, t, J = 7.2 Hz, $-CH_3$), 3.75 (2H, q, J = 7.2 Hz, $-CH_2$), 5.33 (1H, d, J = 2.8 Hz, H–C4), 7.37 (2H, d, J = 7.6 Hz), 7.39 (2H, s, $-NH_2$), 7.41–7.47 (3H, m), 7.60 (2H, d, J = 8.4 Hz), 7.88 (2H, d, J = 8.0 Hz), 7.98 (1H, bs, –NH), 9.44 (1H, bs, –NH) ppm; ^{13}C NMR (100 MHz, DMSO-d_6) δ: 14.4 (CH_3), 55.0 (CH), 60.3 (CH_2), 100.8 (C), 127.2 (CH ×2), 128.0 (CH ×2), 128.8 (CH ×2), 129.4 (CH ×2), 130.1 (CH), 136.0 (C), 144.2 (C), 149.2 (C), 150.6 (C), 153.0 (C═O), 166.1 (C═O) ppm; LC-MS (ESI) (m/z): 402.2 $[M + H]^+$.

*Ethyl 6-phenyl-4-(4-sulfamoylphenyl)-2-thioxo-1,2,3,4-tetrahydropyrimidine-5-carboxylate (**14b**).* Yield 64%; beige solid; mp: 240–241 °C; ^{1}H NMR (400 MHz, DMSO-d_6) δ: 0.77 (3H, t, J = 7.2 Hz, $-CH_3$), 3.79 (2H, q, J = 7.2 Hz, $-CH_2$), 5.37 (1H, d, J = 3.6 Hz, H–C4), 7.37 (2H, d, J = 7.2 Hz), 7.40 (2H, s, $-NH_2$), 7.42–7.50 (3H, m), 7.59 (2H, d, J = 8.4 Hz), 7.90 (2H, d, J = 8.4 Hz), 9.88 (1H, s, –NH), 10.64 (1H, s, –NH) ppm; ^{13}C NMR (100 MHz, DMSO-d_6) δ: 14.4 (CH_3), 54.9 (CH), 60.7 (CH_2), 102.3 (C), 127.3 (CH ×2), 128.1 (CH ×2), 128.8 (CH ×2), 129.8 (CH ×2), 130.3 (CH), 134.9 (C), 144.5 (C), 147.4 (C), 147.6 (C), 165.9 (C═O), 175.7 (C═S) ppm; LC-MS (ESI) (m/z): 418.2 $[M + H]^+$.

*Ethyl 6-(4-fluorophenyl)-2-oxo-4-(4-sulfamoylphenyl)-1,2,3,4-tetrahydropyrimidine-5-carboxylate (**15a**).* Yield 73%; off-white solid; mp: 256–257 °C; ^{1}H NMR (400 MHz, DMSO-d_6) δ: 0.80 (3H, t, J = 6.4 Hz, $-CH_3$), 3.77 (2H, q, J = 6.4 Hz, $-CH_2$), 5.34 (1H, s, H–C4), 7.26 (2H, t, J = 8.0 Hz), 7.38 (2H, s, $-NH_2$), 7.40–7.47 (2H, m), 7.60 (2H, d, J = 7.2 Hz), 7.88 (2H, d, J = 8.0 Hz), 7.98 (1H, bs, –NH), 9.44 (1H, bs, –NH) ppm; ^{13}C NMR (100 MHz, DMSO-d_6) δ: 14.5 (CH_3), 55.0 (CH), 60.4 (CH_2), 101.0 (C), 115.7 (CH ×2, $^2J_{C-F}$ = 21.7 Hz), 127.2 (CH ×2), 128.0 (CH ×2), 131.9 (CH ×2, $^3J_{C-F}$ = 8.4 Hz), 132.2 (C), 144.2 (C), 149.1 (C), 149.6 (C), 152.9 (C═O), 163.6 (C, $^1J_{C-F}$ = 244.2 Hz), 165.9 (C═O) ppm; LC-MS (ESI) (m/z): 418.2 $[M-H]^-$.

*Ethyl 6-(4-fluorophenyl)-4-(4-sulfamoylphenyl)-2-thioxo-1,2,3,4-tetrahydropyrimidine-5-carboxylate (**15b**).* Yield 33%; white solid; mp: 230–231 °C; ^{1}H NMR (400 MHz, DMSO-d_6) δ: 0.82 (3H, t, J = 6.8 Hz, $-CH_3$), 3.81 (2H, q, J = 6.8 Hz, $-CH_2$), 5.37 (1H, d, J = 3.6 Hz, H–C4), 7.27 (2H, t, J = 8.8 Hz), 7.40 (2H, s, $-NH_2$), 7.42–7.46 (2H, m), 7.58 (2H, d, J = 8.0 Hz), 7.89 (2H, d, J = 8.0 Hz), 9.88 (1H, s, –NH), 10.66 (1H, s, –NH) ppm; ^{13}C NMR (100 MHz, DMSO-d_6) δ: 14.5 (CH_3), 54.9 (CH), 60.8 (CH_2), 102.5 (C), 115.7 (CH ×2, $^2J_{C-F}$ = 21.7 Hz), 127.3 (CH ×2), 128.1 (CH ×2), 131.2 (C, $^4J_{C-F}$ = 2.9 Hz), 132.2 (CH ×2, $^3J_{C-F}$ = 8.3 Hz), 144.6 (C), 146.4 (C), 147.6 (C), 163.8 (C, $^1J_{C-F}$ = 245.1 Hz), 165.7 (C═O), 175.6 (C═S) ppm; LC-MS (ESI) (m/z): 436.2 $[M + H]^+$.

*Ethyl 6-(4-chlorophenyl)-2-oxo-4-(4-sulfamoylphenyl)-1,2,3,4-tetrahydropyrimidine-5-carboxylate (**16a**).* Yield 70%; white solid; mp: 260–261 °C; ^{1}H NMR (400 MHz, DMSO-d_6) δ: 0.81 (3H, t, J = 7.2 Hz, –CH_3), 3.78 (2H, q, J = 7.2 Hz, –CH_2), 5.34 (1H, d, J = 2.4 Hz, H–C4), 7.39 (2H, s, –NH_2), 7.40 (2H, d, J = 8.8 Hz), 7.50 (2H, d, J = 8.0 Hz), 7.59 (2H, d, J = 8.0 Hz), 7.87 (2H, d, J = 7.6 Hz), 8.00 (1H, s, –NH), 8.49 (1H, s, –NH) ppm; ^{13}C NMR (100 MHz, DMSO-d_6) δ: 14.5 (CH_3), 55.0 (CH), 60.4 (CH_2), 101.1 (C), 127.2 (CH ×2), 128.0 (CH ×2), 128.9 (CH ×2), 131.5 (CH ×2), 134.6 (C), 134.7 (C), 144.3 (C), 149.0 (C), 149.4 (C), 152.8 (C═O), 165.8 (C═O) ppm; LC-MS (ESI) (m/z): 436.2 $[M + H]^+$.

*Ethyl 6-(4-chlorophenyl)-4-(4-sulfamoylphenyl)-2-thioxo-1,2,3,4-tetrahydropyrimidine-5-carboxylate (**16b**).* Yield 57%; white solid; mp: 265–266 °C; ^{1}H NMR (400 MHz, DMSO-d_6) δ: 0.80 (3H, t, J = 6.8 Hz, –CH_3), 3.78 (2H, q, J = 7.2 Hz, –CH_2), 5.34 (1H, s, H–C4), 7.39–7.42 (4H, m (2H, –NH_2; 2H, ArH)), 7.50 (2H, d, J = 7.6 Hz), 7.59 (2H, d, J = 7.6 Hz), 7.87 (2H, d, J = 8.0 Hz), 8.01 (1H, s, –NH), 9.50 (1H, s, –NH) ppm; ^{13}C NMR (100 MHz, DMSO-d_6) δ: 14.5 (CH_3), 55.0 (CH), 60.4 (CH_2), 101.2 (C), 127.2 (CH ×2), 128.0 (CH ×2), 128.9 (CH ×2), 131.4 (CH×2), 134.8 (C), 144.3 (C), 149.0 (C), 149.4 (C), 152.8 (C), 165.8 (C═O), 176.2 (C═S) ppm; LC-MS (ESI) (m/z): 451.1 $[M–H]^-$.

*2-Oxo-6-phenyl-4-(4-sulfamoylphenyl)-1,2,3,4-tetrahydropyrimidine-5-carboxamide (**17a**).* Yield 75%; white solid; mp: 281–282 °C; ^{1}H NMR (400 MHz, DMSO-d_6) δ: 5.37 (1H, s, H–C4), 6.11 (1H, bs, –NH), 6.82 (1H, bs, –NH), 7.37 (2H, s, –SO_2NH_2), 7.45 (5H, s), 7.59 (2H, d, J = 8.4 Hz), 7.73 (1H, s, –NH), 7.85 (2H, d, J = 8.0 Hz), 8.89 (1H, s, –NH) ppm; ^{13}C NMR (100 MHz, DMSO-d_6) δ: 56.1 (CH), 106.8 (C), 126.9 (CH ×2), 128.3 (CH ×2), 129.3 (CH ×2), 129.7 (CH ×2), 130.3 (CH), 135.1 (C), 141.4 (C), 144.1 (C), 148.8 (C), 153.7 (C═O), 168.7 (C═O) ppm; LC-MS (ESI) (m/z): 373.2 $[M + H]^+$.

*6-Phenyl-4-(4-sulfamoylphenyl)-2-thioxo-1,2,3,4-tetrahydropyrimidine-5-carboxamide (**17b**).* Yield 82%; beige solid; mp: 238–240 °C; ^{1}H NMR (400 MHz, DMSO-d_6) δ: 5.37 (1H, d, J = 3.2 Hz, H–C4), 6.31 (1H, bs, –NH), 6.97 (1H, bs, –NH), 7.38 (2H, s, –SO_2NH_2), 7.46 (5H, s), 7.79 (2H, d, J = 8.4 Hz), 7.87 (2H, d, J = 8.4 Hz), 9.59 (1H, s, –NH), 10.17 (1H, s, –NH) ppm; ^{13}C NMR (100 MHz, DMSO-d_6) δ: 55.9 (CH), 108.5 (C), 127.1 (CH ×2), 128.3 (CH ×2), 129.3 (CH ×2), 130.0 (CH ×2), 130.6 (CH), 134.0 (C), 139.1 (C), 144.4 (C), 147.4 (C), 168.3 (C═O), 175.7 (C═S) ppm; LC-MS (ESI) (m/z): 389.2 $[M + H]^+$.

General procedure for the synthesis of pyrimidintrione-benzenesulfonamides 20 and 21. To an aqueous solution of NaOH (650.0 mg, 6.4 mmol, 3.0 mL), a solution of the suitable pyrimidine-2,4,6(1*H*,3*H*,5*H*)-trione **18–19** (5.0 mmol) in EtOH (5.0 mL) was added slowly at 0 °C. Then, 4-formyl benzenesulfonamide **1** (925.0 mg, 5.0 mmol) in EtOH (5.0 mL) was added dropwise and the mixture was stirred for 16 h at r.t. After completion, the formed precipitate was filtered under vacuum and washed with EtOH and H_2O.

*4-((2,4,6-Trioxotetrahydropyrimidin-5(2H)-ylidene)methyl) benzenesulfonamide (**20**).* Yield 59%; white solid; mp: >300 °C; ^{1}H NMR (400 MHz, DMSO-d_6) δ: 7.55 (2H, s, –NH_2), 7.88 (2H, d, J = 8.0 Hz), 8.07 (2H, d, J = 8.4 Hz), 8.34 (1H, s, CH), 11.34 (1H, s, –NH), 11.51 (1H, s, –NH) ppm; ^{13}C NMR (100 MHz, DMSO-d_6) δ: 122.3 (CH), 126.0 (CH ×2), 133.2 (CH ×2), 137.3 (C), 146.8 (C), 151.3 (C═O), 153.5 (C), 162.3 (C═O), 164.0 (C═O) ppm; LC-MS (ESI) (m/z): 294.0 $[M–H]^-$.

*4-((1,3-Dimethyl-2,4,6-trioxotetrahydropyrimidin-5(2H)-ylidene)methyl)benzenesulfonamide (**21**).* Yield 52%; pale yellow solid; mp: 218–219 °C; ^{1}H NMR (400 MHz, DMSO-d_6) δ: 3.20 (3H, s, –CH_3), 3.28 (3H, s, –CH_3), 7.55 (2H, s, –NH_2), 7.89 (2H, d, J = 8.4 Hz), 8.02 (2H, d, J = 8.4 Hz), 8.43 (1H, s, CH) ppm; ^{13}C NMR (100 MHz, DMSO-d_6) δ: 29.1 (CH_3), 29.7 (CH_3), 122.1 (CH), 128.0 (CH ×2), 132.9 (CH ×2), 137.6 (C), 146.7 (C), 152.2 (C═O), 154.4 (C), 161.1 (C═O), 162.8 (C═O) ppm; LC-MS (ESI) (m/z): 322.0 $[M–H]^-$.

In vitro carbonic anhydrase inhibition assay

An Applied Photophysics stopped-flow instrument was used to evaluate the ability of the test compounds to inhibit the CA-catalyzed CO_2 hydration.[41] Phenol red (at a concentration of 0.2 mM) was used as an indicator, working at the absorbance maximum of 557 nm, with 20 mM HEPES (pH 7.4) as a buffer, and 20 mM Na_2SO_4 (to maintain constant ionic strength), following the initial rates of the CA-catalyzed CO_2 hydration reaction for a period of 10–100 s. The CO_2 concentrations ranged from 1.7 to 17 mM for the assessment of the kinetic parameters and inhibition constants. Enzyme concentrations varied between 5 and 12 nM. For each inhibitor, at least six traces of the initial 5–10% of the reaction were used to determine the initial velocity. The uncatalyzed rates were calculated in the same manner and subtracted from the total observed rates. Stock solutions of each inhibitor (0.1 mM) were prepared in distilled–deionized H_2O and dilutions up to 0.01 nM were done thereafter with the assay buffer. Inhibitor and enzyme solutions were preincubated together for 15 min at r.t. prior to the assay, to allow for the formation of the E–I complex.[44,45] The inhibition constants were obtained by non-linear least-squares methods using PRISM 3 and the Cheng–Prusoff equation as reported earlier[46] and represent the mean from at least three different determinations. hCAs I and II were purchased from Merck, while hCAs VII, IX, and XII are recombinant and obtained in-house.[47,48]

Crystallography

Crystallization and X-ray data collection. The crystal of hCA I was obtained using the hanging drop vapor diffusion method using a 24 well Linbro plate. 2 μL of 10 mg mL^{-1} solution of hCA I in Tris-HCl 20 mM pH 9.0 were mixed with 2 μL of a solution of 28–31% PEG4000, 0.2 M sodium acetate, and 0.1 M Tris pH 8.5–9.0 and were equilibrated against the same solution at 296 K. The complex was prepared by soaking the hCA I native crystals in the mother liquor solution containing **12a** at a concentration of 10 mM for two days. All crystals were flash-frozen at 100 K using a solution

obtained by adding 15% (v/v) glycerol to the mother liquor solution as a cryoprotectant. Data on the crystal of the complex was collected using synchrotron radiation at the XRD2 beamline at Elettra Synchrotron (Trieste, Italy) with a wavelength of 0.971 Å and a DECTRIS Pilatus 6M detector. Data were integrated and scaled using the program XDS.[49] Data processing statistics are shown in ESI.†

Structure determination. The crystal structure of hCA I (PDB ID: 1JV0) without solvent molecules and other heteroatoms was used to obtain initial phases using Refmac5.[50] 5% of the unique reflections were selected randomly and excluded from the refinement data set for Rfree calculations. The initial |Fo − Fc| difference electron density maps unambiguously showed the inhibitor molecules. Refinements proceeded using normal protocols of positional, isotropic atomic displacement parameters alternating with the manual building of the models using COOT.[51] The quality of the final models was assessed with COOT and RAMPAGE.[52] Crystal parameters and refinement data are summarized in Supplementary Information. Atomic coordinates were deposited in the Protein Data Bank (PDB ID: 8QGV). Graphical representations were generated with UCSF Chimera.[53]

Molecular modelling. The three-dimensional structure of the complex between the human carbonic anhydrase XII and a benzenesulfonamide derivative (PDB ID: 6YH9, 1.55 Å resolution)[54] was used to predict the putative binding mode of the pyrimidinone analogues. The complex was submitted to the Protein Preparation Wizard of the Maestro suite (release 2020-3, Schrodinger LLC, 2020) to assign bond orders, refine hydrogen position, and apply a restrained minimization of the resulting structure by using the OPLS3e force field. The structure of the pyrimidinones was built by the 3D Builder module of Maestro and submitted to the LigPrep routine to generate possible tautomers at pH 7.0 ± 1 and metal binding states using Epik software.

For docking calculations, the receptor grid generation routine was applied to specify the location and the size of the grid where the ligands will be docked in suitable poses and orientations. The centroid of the co-crystallized ligand was used to define the grid center, while the overall grid size was based on a ligand diameter midpoint box of 20 × 20 × 20 Å. The hydroxyl groups of Ser, Thr, and Tyr residues within the grid were allowed to rotate during simulations. Flexible and standard-precision docking calculations were performed with post-docking minimization of the resulting complexes. The final docking poses were prioritized based on the corresponding docking score.

Cell culture and proliferation assays

Human MDA-MB-231 cells (ATCC HTB-26, triple-negative breast cancer) and human U87MG (ATCC HTB-14, glioblastoma multiforme) were grown in Dulbecco's modified Eagle's medium (DMEM) supplemented with 10% fetal bovine serum (FBS) (Lonza), 1% penicillin/streptomycin (Lonza), and 1% glutamine (Lonza). Cells were kept at the low passage, returning to their original frozen stocks every 3–4 months. Hypoxic culture conditions were obtained in the presence of 1% O_2 and 5% CO_2. For cell proliferation, 10.000 cells per well were plated in a 48-well plate and treated in 1% FBS with increasing concentrations of **13a**, **17a**, **17b**, **23**, or **SLC-0111**. After 72 h of incubation at 37 °C with 1% O_2 and 5% CO_2, cells were trypsinized and cell counting was performed with a MACSQuant® Analyzer (Miltenyi Biotec).

Interference compound assessment

The behavior of final compounds **10–17a–b**, **20**, **21**, and **23** as pan-assay interference compounds (PAINS)[55] was evaluated through SwissADME.[56,57] JChem for Office (21.15.704, 2023) by ChemAxon[58] was used for structure management, SMILES generation, and file conversion. DHPMs **10–17a–b** and **23** resulted in no PAIN alert, while the software reported an alert for **20** and **21** due to the presence of the barbituric scaffold.

Discussion and conclusion

A series of 15 Biginelli's products (**10–17a–b**, Table 1) decorated with the benzenesulfonamide group, a known CA inhibitor chemotype, along with 2 barbituric compounds (**20–21**, Table 1) were designed and synthesized to better explore the SARs. The compounds' inhibitory activity towards hCAs IX and XII, along with their selectivity over the physiologically relevant hCAs I and II, and the isoform VII was assessed, revealing a low-nanomolar potency and promising isoform selectivity for some compounds. Crystallographic experiments were conducted, allowing the obtainment of the hCA I–**12a** complex with a high resolution (1.84 Å) and a suboptimal Rfree value (0.24). The X-ray structure of the complex with hCA I (PDB ID: 8QGV) helped to gain a fundamental insight into the key interaction networks governing enzyme inhibition. However, attempts to cocrystallize the inhibitor with tumor-associated isoforms failed and docking simulations were performed, revealing the binding pose of **12a** in the catalytic pocket of hCA XII.

Furthermore, derivative **17a**, bearing an amide function in position 5 of the pyrimidindione ring, was one of the most potent and selective compounds against the tumor-associated CAs (in terms of K_I and SI values), and, thus, was used as a hit compound for a preliminary screening campaign of in-house libraries of derivatives (not shown). 2-Aminopyrimidine derivative **23** showed a sufficient structural similarity (AP Tanimoto coefficient ~0.5, calculated by means of the web tool ChemMine),[59,60] to be worthy of investigation. Surprisingly, enzymatic assays of these compounds revealed an unexpectedly high nanomolar potency and selectivity for hCAs IX and XII (Table 1 and Fig. S1†). Thus, representative compounds were selected in the Biginelli series, including **17a**, and pyrimidine **23**, for an *in vitro* investigation of their putative antiproliferative effect on MDA-MB-231 and U87MG

cells. These cell lines have been selected due to the recent evidence of hCA IX overexpression in breast cancer,[43] a disease affecting millions of people annually – with 2.3 million women receiving the diagnosis and more than 600 000 deaths in 2020,[61] and glioblastoma.[22] Compounds **13a** and **23** were effective in reducing the proliferation of the breast cancer cells, with lower IC_{50} values than the reference CA inhibitor **SLC-0111**, and of glioblastoma cells. These results confirm the inhibition of CAs IX and XII as a promising mode of action for anticancer agent development. However, a discrepancy in the activity data was noticed for compound **17a**, probably due to the permeability issues.

Remarkably, the new 2-aminopyrimidine scaffold contained in compound **23** emerged from a preliminary screening based on the chemical similarity of in-house libraries. Although a non-encouraging premise (non-optimal Tanimoto coefficient), **23** displayed high potency and selectivity as a hCA IX and XII inhibitor and a notable antiproliferative effect on breast cancer cells, thereby suggesting it as a valuable starting point for the development of a new derivative library.

Author contributions

The manuscript was written through the contributions of all authors. All authors approved the final version of the manuscript.

Conflicts of interest

There are no conflicts to declare.

Acknowledgements

Hakan Aslan acknowledges the financial support from The Scientific and Technological Research Council of Turkey (TUBITAK) BIDEB-2219 Postdoctoral Research Program (1059B192101059).

References

1 R. L. Siegel, K. D. Miller, N. S. Wagle and A. Jemal, Cancer statistics, 2023, *Ca-Cancer J. Clin.*, 2023, **73**(1), 17–48.
2 Word Health Organization. Cancer [Internet], [cited 2023 Sep 13], Available from: **https://www.who.int/news-room/fact-sheets/detail/cancer**.
3 M. L. Brown, J. Lipscomb and C. Snyder, The burden of illness of cancer: economic cost and quality of life, *Annu. Rev. Public Health*, 2001, **22**, 91–113.
4 M. Wang, M. Chen, X. Wu, X. Huang and B. Yu, CRISPR applications in cancer diagnosis and treatment, *Cell. Mol. Biol. Lett.*, 2023, **28**(1), 73.
5 D. Capoferri, S. Filiberti, J. Faletti, C. Tavani and R. Ronca, Ten Years of CRISPRing Cancers In Vitro, *Cancers*, 2022, **14**(23), 5746.
6 J. Hoeppner, Robotic Cancer Surgery, *Cancers*, 2021, **13**(19), 4931.
7 A. Hoeben, E. A. J. Joosten and M. H. J. van den Beuken-van Everdingen, Personalized Medicine: Recent Progress in Cancer Therapy, *Cancers*, 2021, **13**(2), 242.
8 L. Falzone, S. Salomone and M. Libra, Evolution of Cancer Pharmacological Treatments at the Turn of the Third Millennium, *Front. Pharmacol.*, 2018, **9**, 1300.
9 Z. Fu, L. Wang, S. Li, F. Chen, K. K. W. Au-Yeung and C. Shi, MicroRNA as an Important Target for Anticancer Drug Development, *Front. Pharmacol.*, 2021, **12**, 736323.
10 Y. You, X. Lai, Y. Pan, H. Zheng, J. Vera and S. Liu, *et al.*, Artificial intelligence in cancer target identification and drug discovery, *Signal Transduction Targeted Ther.*, 2022, **7**(1), 1–24.
11 C. T. Supuran, A simple yet multifaceted 90 years old, evergreen enzyme: Carbonic anhydrase, its inhibition and activation, *Bioorg. Med. Chem. Lett.*, 2023, **93**, 129411.
12 *Metalloenzymes: From Bench to Bedside*, ed. C. T. Supuran and W. A. Donald, Academic Press - Elsevier Science Publishing Co Inc, 1st edn, 2023, p. 643.
13 C. T. Supuran, Novel carbonic anhydrase inhibitors, *Future Med. Chem.*, 2021, **13**(22), 1935–1937.
14 A. Kumar, K. Siwach, C. T. Supuran and P. K. Sharma, A decade of tail-approach based design of selective as well as potent tumor associated carbonic anhydrase inhibitors, *Bioorg. Chem.*, 2022, **126**, 105920.
15 H. O. Tawfik, A. Petreni, C. T. Supuran and M. H. El-Hamamsy, Discovery of new carbonic anhydrase IX inhibitors as anticancer agents by toning the hydrophobic and hydrophilic rims of the active site to encounter the dual-tail approach, *Eur. J. Med. Chem.*, 2022, **232**, 114190.
16 C. T. Supuran, Targeting carbonic anhydrases for the management of hypoxic metastatic tumors, *Expert Opin. Ther. Pat.*, 2023, 1–20.
17 A. Nocentini and C. T. Supuran, Carbonic anhydrase inhibitors as antitumor/antimetastatic agents: a patent review (2008-2018), *Expert Opin. Ther. Pat.*, 2018, **28**(10), 729–740.
18 A. Angeli, F. Carta, A. Nocentini, J. Y. Winum, R. Zalubovskis and A. Akdemir, *et al.*, Carbonic Anhydrase Inhibitors Targeting Metabolism and Tumor Microenvironment, *Metabolites*, 2020, **10**(10), 412.
19 P. C. McDonald, S. C. Chafe, C. T. Supuran and S. Dedhar, Cancer Therapeutic Targeting of Hypoxia Induced Carbonic Anhydrase IX: From Bench to Bedside, *Cancers*, 2022, **14**(14), 3297.
20 S. Kalinin, A. Malkova, T. Sharonova, V. Sharoyko, A. Bunev and C. T. Supuran, *et al.*, Carbonic Anhydrase IX Inhibitors as Candidates for Combination Therapy of Solid Tumors, *Int. J. Mol. Sci.*, 2021, **22**(24), 13405.
21 J. Y. Winum, M. Rami, A. Scozzafava, J. L. Montero and C. Supuran, Carbonic anhydrase IX: a new druggable target for the design of antitumor agents, *Med. Res. Rev.*, 2008, **28**(3), 445–463.
22 F. Liguori, S. Carradori, R. Ronca, S. Rezzola, S. Filiberti and F. Carta, *et al.*, Benzenesulfonamides with different rigidity-conferring linkers as carbonic anhydrase inhibitors: an

insight into the antiproliferative effect on glioblastoma, pancreatic, and breast cancer cells, *J. Enzyme Inhib. Med. Chem.*, 2022, **37**(1), 1857–1869.

23 S. Mussi, S. Rezzola, P. Chiodelli, A. Nocentini, C. T. Supuran and R. Ronca, Antiproliferative effects of sulphonamide carbonic anhydrase inhibitors C18, SLC-0111 and acetazolamide on bladder, glioblastoma and pancreatic cancer cell lines, *J. Enzyme Inhib. Med. Chem.*, 2022, **37**(1), 280–286.

24 I. Koyuncu, E. Temiz, M. Durgun, A. Kocyigit, O. Yuksekdag and C. T. Supuran, Intracellular pH-mediated induction of apoptosis in HeLa cells by a sulfonamide carbonic anhydrase inhibitor, *Int. J. Biol. Macromol.*, 2022, **201**, 37–46.

25 C. B. Mishra, R. K. Mongre, A. Prakash, R. Jeon, C. T. Supuran and M. S. Lee, Anti-breast cancer action of carbonic anhydrase IX inhibitor 4-[4-(4-Benzo[1,3]dioxol-5-ylmethyl-piperazin-1-yl)-benzylidene-hydrazinocarbonyl]-benzenesulfonamide (BSM-0004): in vitro and in vivo studies, *J. Enzyme Inhib. Med. Chem.*, 2021, **36**(1), 954–963.

26 S. C. Chafe, F. S. Vizeacoumar, G. Venkateswaran, O. Nemirovsky, S. Awrey and W. S. Brown, *et al.*, Genome-wide synthetic lethal screen unveils novel CAIX-NFS1/xCT axis as a targetable vulnerability in hypoxic solid tumors, *Sci. Adv.*, 2021, **7**(35), eabj0364.

27 P. C. McDonald, S. Chia, P. L. Bedard, Q. Chu, M. Lyle and L. Tang, *et al.*, A Phase 1 Study of SLC-0111, a Novel Inhibitor of Carbonic Anhydrase IX, in Patients With Advanced Solid Tumors, *Am. J. Clin. Oncol.*, 2020, **43**(7), 484–490.

28 British Columbia Cancer Agency, An Open-label, Multi-center, Phase 1b Study to Investigate the Safety and Tolerability of SLC-0111 (WBI-5111) in Combination With Gemcitabine in Metastatic Pancreatic Ductal Adenocarcinoma Subjects Positive for Carbonic Anhydrase IX [Internet], 2023 [cited 2023 Sep 12], Available from: **https://clinicaltrials.gov/study/NCT03450018**.

29 P. Biginelli, Derivati Aldeiduredici Degli Eteri Acetile Dossal-Acetico, *Gazz. Chim. Ital.*, 1893, **23**(1), 360–413.

30 H. G. O. Alvim, E. N. da S. Júnior and B. A. D. Neto, What do we know about multicomponent reactions? Mechanisms and trends for the Biginelli, Hantzsch, Mannich, Passerini and Ugi MCRs, *RSC Adv.*, 2014, **4**(97), 54282–54299.

31 Á. Cores, J. Clerigué, E. Orocio-Rodríguez and J. C. Menéndez, Multicomponent Reactions for the Synthesis of Active Pharmaceutical Ingredients, *Pharmaceuticals*, 2022, **15**(8), 1009.

32 X. Lei, P. Lampiri, P. Patil, G. Angeli, C. G. Neochoritis and A. Dömling, A multicomponent tetrazolo indole synthesis, *Chem. Commun.*, 2021, **57**(54), 6652–6655.

33 M. Thomaidi, L. E. Vagiaki, N. P. Tripolitsiotis, G. K. Angeli, T. Zarganes-Tzitzikas and K. Sidiropoulou, *et al.*, Local Anesthetics via Multicomponent Reactions, *ChemMedChem*, 2022, **17**(15), e202200246.

34 S. Kalinin, A. Nocentini, A. Kovalenko, V. Sharoyko, A. Bonardi and A. Angeli, *et al.*, From random to rational: A discovery approach to selective subnanomolar inhibitors of human carbonic anhydrase IV based on the Castagnoli-Cushman multicomponent reaction, *Eur. J. Med. Chem.*, 2019, **15**(182), 111642.

35 G. C. Tron, A. Minassi and G. Appendino, Pietro Biginelli: The Man Behind the Reaction, *Eur. J. Org. Chem.*, 2011, **2011**(28), 5541–5550.

36 A. Angeli, E. Trallori, M. Ferraroni, L. Di Cesare Mannelli, C. Ghelardini and C. T. Supuran, Discovery of new 2, 5-disubstituted 1,3-selenazoles as selective human carbonic anhydrase IX inhibitors with potent anti-tumor activity, *Eur. J. Med. Chem.*, 2018, **157**, 1214–1222.

37 S. J. Lin, W. J. Tsai, W. F. Chiou, T. H. Yang and L. M. Yang, Selective COX-2 inhibitors. Part 2: Synthesis and biological evaluation of 4-benzylideneamino- and 4-phenyliminomethyl-benzenesulfonamides, *Bioorg. Med. Chem.*, 2008, **16**(5), 2697–2706.

38 K. A. Dilmaghani, B. Zeynizadeh and M. Amirpoor, Ultrasound-Mediated Synthesis of 3,4-Dihydropyrimidin-2-(1H)-Ones (or Thiones) with NaHSO4·H2O, *Phosphorus, Sulfur Silicon Relat. Elem.*, 2013, **188**(11), 1634–1642.

39 A. Herschhorn, L. Lerman, M. Weitman, I. O. Gleenberg, A Nudelman and A. Hizi, De Novo Parallel Design, Synthesis and Evaluation of Inhibitors against the Reverse Transcriptase of Human Immunodeficiency Virus Type-1 and Drug-Resistant Variants, *J. Med. Chem.*, 2007, **50**(10), 2370–2384.

40 S. E. Motika, R. J. Ulrich, E. J. Geddes, H. Y. Lee, G. W. Lau and P. J. Hergenrother, Gram-Negative Antibiotic Active Through Inhibition of an Essential Riboswitch, *J. Am. Chem. Soc.*, 2020, **142**(24), 10856–10862.

41 R. G. Khalifah, The carbon dioxide hydration activity of carbonic anhydrase. I. Stop-flow kinetic studies on the native human isoenzymes B and C, *J. Biol. Chem.*, 1971, **246**(8), 2561–2573.

42 C. T. Supuran, Exploring the multiple binding modes of inhibitors to carbonic anhydrases for novel drug discovery, *Expert Opin. Drug Discovery*, 2020, **15**(6), 671–686.

43 V. Ciccone, A. Filippelli, A. Angeli, C. T. Supuran and L. Morbidelli, Pharmacological Inhibition of CA-IX Impairs Tumor Cell Proliferation, Migration and Invasiveness, *Int. J. Mol. Sci.*, 2020, **21**(8), 2983.

44 I. D'Agostino, G. E. Mathew, P. Angelini, R. Venanzoni, G. Angeles Flores and A. Angeli, *et al.*, Biological investigation of N-methyl thiosemicarbazones as antimicrobial agents and bacterial carbonic anhydrases inhibitors, *J. Enzyme Inhib. Med. Chem.*, 2022, **37**(1), 986–993.

45 S. Carradori, A. Angeli, P. S. Sfragano, X. Yzeiri, M. Calamante and D. Tanini, *et al.*, Photoactivatable Heptamethine-Based Carbonic Anhydrase Inhibitors Leading to New Anti-Antibacterial Agents, *Int. J. Mol. Sci.*, 2023, **24**(11), 9610.

46 I. D'Agostino, S. Zara, S. Carradori, V. DeLuca, C. Clemente and C. H. M. Kocken, *et al.*, Antimalarial Agents Targeting Plasmodium Falciparum Carbonic Anhydrase: Towards Dual Acting Artesunate Hybrid Compounds, *ChemMedChem*, 2023, e202300267.

47 A. Redij, S. Carradori, A. Petreni, C. T. Supuran and M. P. Toraskar, Coumarin-pyrazoline Hybrids as Selective Inhibitors of the Tumor-associated Carbonic Anhydrase IX and XII, *Anti-Cancer Agents Med. Chem.*, 2023, **23**(10), 1217–1223.

48 A. Sethi, S. Munagalasetty, M. Arifuddin, S. Carradori, C. T. Supuran and R. Alvala, *et al.*, Coumarin and Piperazine Conjugates as Selective Inhibitors of the Tumor-associated Carbonic Anhydrase IX and XII Isoforms, *Anti-Cancer Agents Med. Chem.*, 2023, **23**(10), 1184–1191.

49 A. G. W. Leslie and H. R. Powell, Processing diffraction data with mosflm, in *Evolving Methods for Macromolecular Crystallography*, ed. R. J. Read and J. L. Sussman, Springer Netherlands, Dordrecht, 2007, pp. 41–51, (NATO Science Series).

50 G. N. Murshudov, A. A. Vagin and E. J. Dodson, Refinement of macromolecular structures by the maximum-likelihood method, *Acta Crystallogr., Sect. D: Biol. Crystallogr.*, 1997, **53**(Pt 3), 240–255.

51 P. Emsley, B. Lohkamp, W. G. Scott and K. Cowtan, Features and development of Coot, *Acta Crystallogr., Sect. D: Biol. Crystallogr.*, 2010, **66**(Pt 4), 486–501.

52 S. C. Lovell, I. W. Davis, W. B. Arendall III, P. I. W. de Bakker, J. M. Word and M. G. Prisant, *et al.*, Structure validation by Cα geometry: ϕ,ψ and Cβ deviation, *Proteins: Struct., Funct., Bioinf.*, 2003, **50**(3), 437–450.

53 E. F. Pettersen, T. D. Goddard, C. C. Huang, G. S. Couch, D. M. Greenblatt and E. C. Meng, *et al.*, UCSF Chimera–a visualization system for exploratory research and analysis, *J. Comput. Chem.*, 2004, **25**(13), 1605–1612.

54 J. Smirnovienė, A. Smirnov, A. Zakšauskas, A. Zubrienė, V. Petrauskas and A. Mickevičiūtė, *et al.*, Switching the Inhibitor-Enzyme Recognition Profile via Chimeric Carbonic Anhydrase XII, *ChemistryOpen*, 2021, **10**(5), 567–580.

55 J. B. Baell and J. W. M. Nissink, Seven Year Itch: Pan-Assay Interference Compounds (PAINS) in 2017—Utility and Limitations, *ACS Chem. Biol.*, 2018, **13**(1), 36–44.

56 A. Daina, O. Michielin and V. Zoete, SwissADME: a free web tool to evaluate pharmacokinetics, drug-likeness and medicinal chemistry friendliness of small molecules, *Sci. Rep.*, 2017, **7**(1), 42717.

57 SwissADME [Internet], [cited 2023 Sep 14], Available from: **http://www.swissadme.ch/**.

58 Chemaxon [Internet], [cited 2023 Sep 14], Available from: **https://chemaxon.com**.

59 ChemMine Tools [Internet], [cited 2023 Sep 14], Available from: **https://chemminetools.ucr.edu/**.

60 T. W. Backman, Y. Cao and T. Girke, ChemMine tools: an online service for analyzing and clustering small molecules, *Nucleic Acids Res.*, 2011, **39**, W486–W491.

61 Word Health Organization, Breast cancer [Internet], [cited 2023 Sep 13], Available from: **https://www.who.int/news-room/fact-sheets/detail/breast-cancer**.